Design of a new sensor to improve accuracy of ECT images

Z. Liu, L. Babout, R. Banasiak, D. Sankowski

Computer Engineering Department, Technical University of Łódź, Poland, liuz@kis.p.lodz.pl

Reviewer: W.Q. Yang (University of Manchester, UK)

Summary: Electrical capacitance tomography (ECT) has been successfully applied in many industrial fields. However, the resolution of ECT still needs to be improved so that it can be used in a wider scope. As a first attempt to overcome this drawback, a new design is presented as a prototype system for improving the resolution based on rotation of the sensor. By keeping the number of electrodes constant, the image quality may be enhanced by making additional measurements at different angles.

Keywords: ECT sensor, Rotatable Sensor, Improved resolution, Image Reconstruction

1. Introduction

Electrical capacitance tomography is a method for determination of the dielectric permittivity distribution in the interior of a subject from capacitance measurements. It is based on the use of an array of electrodes mounted around a pipe or the reactor circumference. And ECT system normally consists of a capacitance sensor, a capacitance measuring unit and a control computer as shown in Fig. 1.

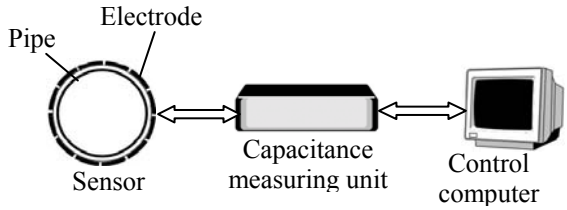

Fig. 1. ECT system

In recent years, developments in the technology have led to wide use of ECT for industrial applications for monitoring, measurement and control (Yang, 2007). Because of the limitation in image resolution, however, its application is still limited in a certain extent, while some applications may require higher spatial resolution.

A practicable solution to improve image resolution is to enhance the independent measurements for each frame. The number of electrodes in an ECT sensor is usually 8 or 12. Increasing the number of electrodes can increase the available data and therefore possibly improve the measurement accuracy. However, a large number of electrodes would result in difficulties e.g. complicated and expensive hardware, smaller capacitance to be measured and a slower data acquisition rate (Yang, 2006a). Recent research has concluded that more electrodes may not necessarily give better images because of worse singularity with more electrodes (Yang, 2006b). In addition, the pipe wall of an ECT sensor capacity can only support a limited number of electrodes even if placed on multi-planes. For a given diameter and electrode area, more electrodes are enwound around the pipe, longer electrodes are required, and hence the sensor will have a larger averaging area.

To overcome the problem of limited spatial resolution, a new rotatable sensor has been designed and presented in this paper.

2. Sensor

In the new ECT sensor, no more electrodes are added in the sensor. The system is shown in Fig. 2.

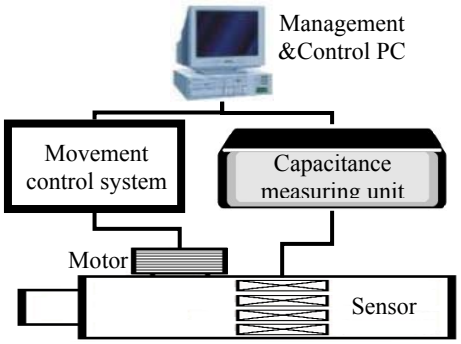

Fig. 2. Rotatable ECT system

The system is composed of a capacitance sensor, a capacitance measuring unit, a movement control unit and a control computer. The movement control unit is used to control the movement and position of the rotatable parts of the sensor driving by a motor.

The structure of the sensor is shown in Fig. 3. It is composed of a single plane of external electrodes. Electrodes are located on the same plane around a boundary of imaged area. The major difference is that the new sensor allows rotation of the electrodes around the object of investigation in order to increase the number of capacitance measurements with a fixed number of electrodes.

For low weight and strong structure, high performance aluminium alloy material is selected for the major frame of the mechanical system.

The tubes have a negative effect on the measurement of the internal capacitance because the wall capacitance is effectively in series with the internal capacitance. The thinner wall gives better sensor performance. However, if the wall is too thin, it cannot support the weight of the sensor. Usually, the thickness of sensor wall is between 2 and 4 mm (Yang, 2006a). The key dimensions of the mechanical parts are listed in Table 1.

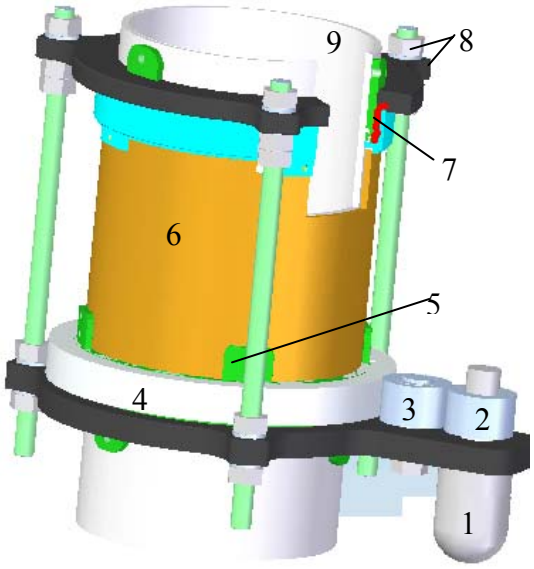

Fig. 3. The assembly view of the sensor; 1. Stepper motor, 2.Driver gear, 3. Intermediate gear, 4. Transmission gear, 5. Support mechanism, 6. Cylindrical tube 7. Bearing, 8.Fix mechanism, 9. Inner tube

*Table 1. Dimension of the mechanical parts. *from Fig.3*

Part name	Type	Dimension (mm)
Cylindrical tube 6*	Inner	150.5
	Outer	154
Inner tube 9*	Inner	150
	Outer	146

The electrodes are mounted on an insulating tube 6, which overlays on tube 9. Between tube 6 and tube 9, sliding bearings 7 are added to reduce friction between the two tubes so that the outer tube can rotate easily. The electrodes are surrounded by an earthed outer screen to minimise the interference of external fields or objects. To avoid the possible buildup of electrostatic charges, a low permittivity material with excellent lubricant performance is used to fill the gap between the two tubes. Because Teflon and Vaseline have a low permittivity, which is very close to the permittivity (2.2) of PP tube, and the two materials also have a low friction, as show in Table 2, one of the materials is selected as the insulated material after comparison and test in the prototype system.

Table 2. Normal low permittivity materials

Material	Relative Permittivity ($x\varepsilon_0$)	Friction
Teflon	2.1	0.04
Vaseline	2.16	0.075

With the drive of stepper motor *1*, the larger gear *4* is propelled with a shifted rotating speed by the smaller gear *2* and intermediate gear *3*, and then the movement is transferred to the support of sensor *5*, which brings along the rotation of the tube 6. The movement of the cylindrical tube is synchronised with the motor. Any change of the motor's position will lead to the movement of the sensor.

The movement is by a continuously variable motor with a digital control module, which drives the rotation of the overlaying tube *6* with a given impulse signal. The capacitance measurements of the media contained within the inner tube are obtained at different stepper angle until one electrode in the outer tube coincides with the previous position of its right side neighbour electrode.

To verify that overlaying tube does not affect greatly the quality of the images, measurements were taken as show in Fig. 4. Note that the tube dimensions are slightly different from those listed in Table 1 (Inner tube: Φ_{outer} = 150mm, Φ_{inner} = 142mm; Outer tube: Φ_{outer} = 160mm, Φ_{inner} = 54mm).

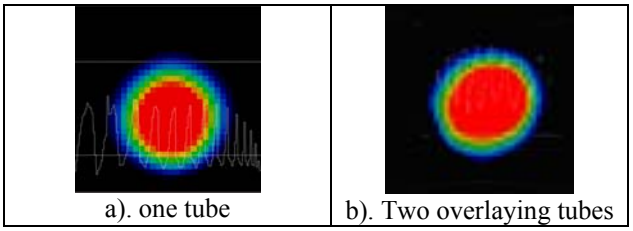

Fig. 4. Measurement result with two tubes

It is important for the inner tube to be concentric as precisely as possible with the outer one. The image was distorted when overlaying tube is mounted because it is difficult to keep the two tubes concentric without special equipment. The smaller the clearance between the two tubes the better the result. However, the mechanical movement needs a necessary clearance so that the sensor could rotate easily. The mechanical clearance is 0.5 mm~1.0 mm.

3. Movement control

A stepper motor is used in the system to move the sensor, including a drive actuator and a synchronous motor with a high number of poles. The advantages of the motor are high holding torque and very good positioning. Individual steps or partial steps can be approached directly through control of the stator windings in full step or micro-step mode. The stepper motor can work in an excellent status in a wide speed range from 0 to 300 rpm.

The stepper motor drive system is shown in Fig. 5. The software interface will be designed to allow a user to input parameters such as speed, direction and time. Such information will be converted into impulse signals by the movement driver. After the impulse signal is subdivided and amplified according to the logic relation, it will drive the motor.

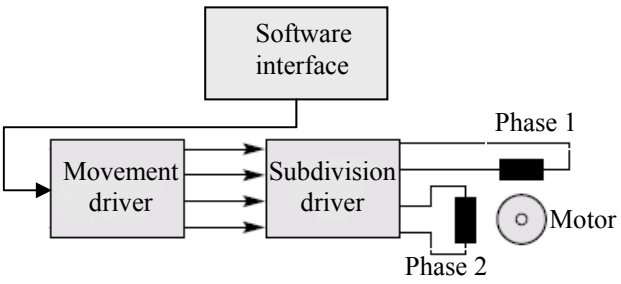

Fig. 5. Block scheme of the stepper motor driver

The number of measurements for N-electrodes is given by equation (1) with binomial coefficient when electrode pairs are taken without taking into account the electrode order in pair.

$$M = \frac{N(N-1)}{2} \qquad (1)$$

The present work is based on a sensor with 16 electrodes. The number of measurements is 120 according to equation (1). Based on this value, the number of step angles and corresponding acquisition time of the corresponding rotatable sensor can be calculated, as given in table 3. From table 3, the number of new measurements is relatively close to the normal number of measurements required with a larger number of electrodes.

Table 3. Measurement analysis. n is the number of rotation positions

N-Channel ECT	Total data (N*(N-1)/2)	Rotatable ECT 16Channels) n positions	Data (n*M)
16	120	1	120
32	496	4	480
64	2080	16	1920
128	8128	64	7680
256	32640	256	30720

For a rotatable sensor with *16*-channel electrodes, $4^{\wedge(\alpha-1)}$ *(*α*= 2, 3...)* rotation positions are required to obtain a number of measurement set of the same order as a conventional sensor with *16*α-channel electrodes.

If the measurement time of each frame is *t* ms, the electrodes must rotate from one position to the previous position of its right side neighbour electrode with a *22.5°* angle within *p*t* ms (*p* means the total number of angle positions). Consequently, the revolving speed of the sensor can be calculated:

$$\omega = \frac{62.5}{p*t}\ \text{r/s} = \frac{3750}{p*t}\ \text{r/min.} \qquad (2)$$

Based on Table 3, the rotation speed will be at its maximum when the number of rotation positions is 4. The present 16-electrodes ECT system allows single measurement for electrode pair to be acquired in *20* ms. According to equation (2), the maximum rotation speed will be about *45 r/min* when *4* step angles are set, which is easily achievable with the selected stepper motor and appropriate choice of intermediate gear diameters (see Fig. 3).

The main drawback of this sensor design is that it is difficult to provide real time measurements. It is obvious that acquiring more data set will need more time. An issue is to estimate what is the maximum flow speed that can be considered acceptable to legitimate the capacitance measurements in dynamic mode from the rotatable sensor. If the media is not too perturbed (near-stationary) the flow portion alongside the length of the electrodes does not change significantly. Based on this assumption, a portion of the media which is contained in the first half of the electrodes length will not change in the second half. The electrode length is mostly limited by the smallest capacitance value that can be measured by a capacitance measuring circuit. Shorter electrodes provide better dynamics but lower capacitance. With a large diameter ECT sensor, say 10 cm, the electrode length is typically 10 cm (Yang, 2006a). For electrodes with length of 16cm fixed, 4 angle steps with 20 ms acquisition time each (equivalent to nearly 32 electrodes), the maximum flow rate is then around 1m/s. From table 4, it is possible for the sensor in dynamic mode to be applied in many multi-phase measurements since the flow speed of liquid is less than *1.0*.

Table 4. Normal liquid flow speed statistics

Flow type	Speed(m/s)
Tap water	0.5~1.1
Free canalization water	0~1.0
Low viscosity liquid	1.5~3.0
High viscosity liquid	0.1~1.0

4. Image reconstruction algorithm: a possible strategy

Image reconstruction is a key issue since the new acquisition strategy involves a modification to the usual inverse/forward methods.

Image reconstruction is defined as obtaining the material parameter distribution from measurement vector. It can be expressed in mathematical form as:

$$b : V \mapsto R \qquad (3)$$

Where R is the reconstructed material parameter distribution, V is the measurement vector (real or simulated).

The linear back projection algorithm (Williams, 1995) can be applied in the new rotatable ECT system. Suppose the sensor with N-electrodes rotated p times ($p=4^{\wedge(\alpha-1)}$ (α=2, 3…)), then formula *3* can be described in matrix form:

$$g = S'C' \qquad (4)$$

Where:

$g \in RL \times 1$, representing the grey level of a L-pixel image approximating the distribution of dielectric properties in the sensing area;

$C' \in R^{pM \times 1}$ vector, it is interrelated to the vector of $C_k \in R^{M \times 1}$ (k = 1…, p), C_k represents the *M*

measurements in the *k*th angle position taken from the rotatable ECT system. The following can be used to rearrange pM electrode pairs:

$$\{(m);\ m=1,\ M,\ M+1,...,pM\} \Leftrightarrow$$
$$\{(p_\theta,i,j);\ p_i=1,\ldots,p;\ i=1,\ldots,N\text{-}1;j=i+1,\ldots,N\} \quad (5)$$

For N electrodes pairs of the p_θth position for the *i*th electrode

$$C'_{p\theta,i}=\{(p_\theta, i, j);\ j=i+1,\ \ldots,\ N\} \quad (6)$$

After rearranging the pM electrode pairs in a sequence that is equivalent to a sensor with αN-electrode by putting equation (6) into C,

$$C=\{(C'_{p\theta,i});\ p_\theta=1,\ldots,p;\ i=1,\ \ldots,\ N\} \quad (7)$$

S' is an $L\times pM$ matrix, the meaning of which can be described by partitioning it in the following way:

$$S'=[s_{(1)}\ldots s_M\ s_{M+1}\ldots s_{(pM)}] \quad (8)$$

where $s_{(i)}(i=1,...,pM)$ is a $L\times 1$ vector. At each position, S' is recalculated. By employing the Landweber iteration which is regarded as the most reliable iterative algorithm by many researchers:

$$g_{k+1}=g_k+\alpha_k S'^{T}(C'-S'g_k) \quad (9)$$

Where g_k is the image in the *k*th step, α_k is the relaxation factor in the *k*th step.

If the spatial sensitivity distribution *S* is known, the image reconstruction process is just a simple vector-matrix multiplication and iteration.

5. Rotatable ECT sensor Simulation

In order to verify whether the image of new rotatable sensor is improved, a simulation based on FEM was performed. Linear forward problem was used to calculate capacitances on the basis of the actual reconstructed permittivity distribution. Linear Back Projection (LBP) was used to reconstruct the phantom image(By equation *4*), and by Landweber Iterations(LI) method to obtained the more sharpen image(By equation *9*). FEM was applied to solve forward problem for the initial simulated images as well as for the phantom.

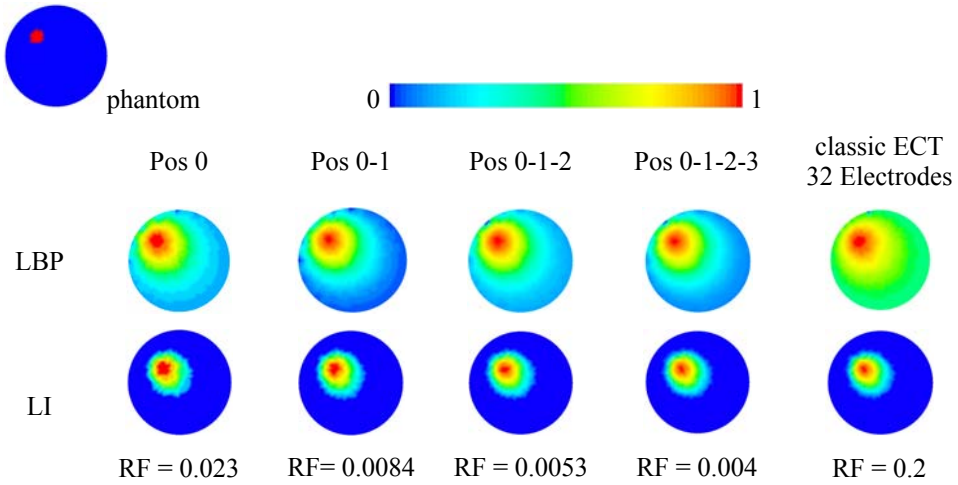

Fig. 6. Comparison of the image for the rotatable Sensor in different position with classic Sensor. LI- Landweber Iterations and iterations times=20. Pos 0 means the image was reconstructed based on a 16-electrodes sensor, Pos0-1-...-i means the image was reconstructed based on merging the measurement data of pos 1 to pos i of the 16-electrodes sensor, RF is relaxation factor.

The example phantom was used to study the new approach and give some comparison between classic 32 electrodes ECT sensor and the new rotatable approach. Examples of the reconstructed images are presented in Fig. 6. For each position, the sensitivity matrix was recalculated. The measurement data set from former position was reused for the image reconstruction in the later position. The preliminary results shows that the increase of position of the rotatable led to improvement in capacitance imaging. When the sensor rotated up to the 4th position, the image quality is almost comparable to an image obtained with a classical 32-electrodes ECT sensor.

6. Conclusion

The paper presented a new ECT sensor to improve the spatial resolution. A rotatable sensor with 16 in-plane electrodes has been considered. The number of electrodes may vary in the future, depending on the pipe diameter, on which the sensor will be fixed. The first prototype is being made. Preliminary tests have been carried out on static objects before considering multi-phase flows. The prototype will be designed to be mounted on a flow apparatus (multi-phase flow, pneumatic conveyor) which is in its final stage of construction at the Computer Engineering Department of the Technical University of Lodz.

Acknowledgement

The work is funded by the European Community's Sixth Framework Programme – Marie Curie Transfer of Knowledge Action (DENIDIA, contract No.: MTKD-CT-2006-039546). The work reflects only the author's views and the European Community is not liable for any use that may be made of the information contained therein. The authors also would like to thank Dr Radosław Wajman, Dr Krzysztof Grudzień and Dr Andrzej Romanowski for their help.

REFERENCE

WILLIAMS R.A., BECK M., (1995), *Process Tomography: Principles, Techniques and Applications*, Butterworth-Heinemann Ltd, Oxford.

YANG M., (2007), *Development of new generation electrical capacitance tomography system and application for milk flow metering*, PhD thesis, The University of Manchester.

YANG W. ,(2006b), Latest developments and new challenges in ECT, 4th International Symposium on Process Tomography, Warsaw 2006, pp 1-4.

YANG W., (2006a), Key issues in designing capacitance tomography sensors, *IEEE sensors*, pp 497-505.